

Laser Ablation in Bilayer Film/Substrate System

11/10/2017

1 Introduction

The concepts of Radice et al's laser ablation model are applied here to a two-layer system consisting of film and PMMA substrate. The concepts employed by Radice et al to predict phase change are adapted here. In this model, the laser is pulsed and heat accumulates between pulses in the system. Furthermore, irradiance reflected off the interface into the PMMA is accounted for, and irradiance absorbed by the substrate is computed as well.

2 Geometry and Coordinates

The carbon steel substrate is assigned a thickness of x_s (m) and the PMMA film is assigned time-dependent thickness $x_f(t)$ (m). The PMMA is assigned an initial thickness $x_f(0)$. The material interface is taken to be at $x = 0$. The laser is taken to be above the PMMA and its beam is directed in the $-x$ direction (Figure 1).

The domain was given a coarse mesh spacing ($1E-7$ m) in the substrate. However, the large amount of energy introduced by the laser required fine ($1E-9$ m) meshing in the PMMA.

3 Boundary Conditions and Initial Condition

The temperature was set to a constant $25^\circ C$ initially.

An insulated boundary condition was applied at $x = -x_s$. To apply the methodology of Radice et al, incoming laser radiation at $x = x_f(0)$ was

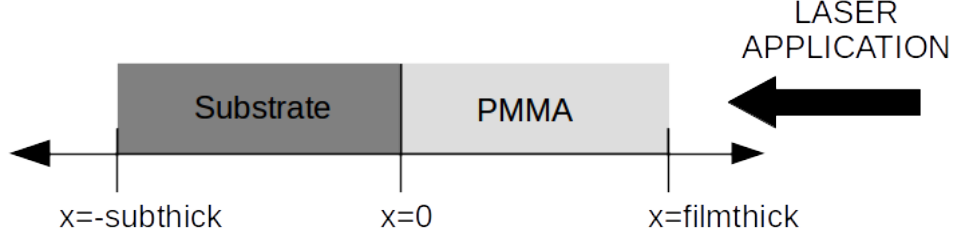


Figure 1: Coordinates for the two-material laser ablation model.

applied as a flux. As the laser radiation hits the top surface of the PMMA at $x = x_f$, total irradiance entering the PMMA is

$$I(x_f, t) = I_0(1 - R_f)F(t) \quad (1)$$

where I_0 is peak irradiance of the pulse, R_f is the reflectivity of the PMMA, and $F(t)$ is the function describing the triangular waveform given by Ahn et al.

However, not all the irradiance is absorbed by the PMMA. In other words, not all the energy described by Equation 1 goes into the PMMA on the first pass. At the PMMA/substrate interface, the remaining flux of laser irradiance is dependent on $x_f(t)$, the remaining thickness of PMMA:

$$I(0, t) = I_0 * (1 - R_f)F(t)e^{-\alpha_f x_f(t)} \quad (2)$$

Therefore, the amount of energy available for first pass heating must be less than that in Eq. 1. This first-pass heating due to laser radiation is approximated as a surface flux by subtracting Eq. 3 from Eq. 1:

$$I(x_f, t) = I_0(1 - r_f)F(t)(1 - e^{-\alpha_f x_f(t)}) \quad (3)$$

Equation 3 is applied as the right-hand boundary condition in the model and accounts for the energy absorbed by the PMMA on the first pass. Treating the first pass as a surface flux is justified by Radice et al, who consider PMMA a surface absorber at 1070 nm.

4 Source Term

The second-pass heating in the PMMA, which results from radiation reflected off the substrate, is computed as a source term:

$$S(x, t) = I(0, t)R_{sub}(\alpha_p)\exp(-\alpha_p x); \quad x > 0 \quad (4)$$

Laser heating in the substrate is also computed as a source term:

$$S(x, t) = I(0, t)(1 - r_{sub}) \times \exp(\alpha_s x); \quad x \leq 0 \quad (5)$$

5 Material Properties

The work of Radice et al is adapted here to incorporate latent heat of phase change. As the material is heated, specific heat is increased once the material begins its phase change and then set to the specific heat of vapor once the phase change is complete. The increase in specific heat, when integrated over the temperature range of phase transition, must account for the latent heat of phase change. For more information, see section 3.4 in Radice et al.

After phase change, the material's density and specific heat are changed to that of air/vapor. Thermal conductivity is increased by several orders of magnitude, effectively applying the laser flux boundary condition (Eq. 3 to unvaporized film material as the heat "passes through" the vaporized material.

For a temperature $T1$ where phase change begins and a temperature $T2$ where phase change ends, and material of temperature $T(x, t)$, equations that assign material properties as described above are:

$$k(x, t) = k_s + 1E5 \times H(T(x, t) - T2) \quad (6)$$

where H is the heaviside step function. For this model, k_s is the conduction coefficient of liquid oil. Thus, Eq. 6 increases k by several orders of magnitude once $T(x)$ surpasses $T2$. Note that this relation is not employed for the substrate. It is assumed that only the film will undergo phase change.

Specific heat $C(x, t)$ of the film must also be increased during phase change, i.e. while $T1 \leq T \leq T2$. To achieve this, the formula for material property is

$$C(x, t) = C_{P,s} \times H(T2 - T(x, t)) + \frac{\Delta h}{T2 - T1} \times H(T(x, t) - T1) \times H(T2 - T(x, t)) \quad (7)$$

where Δh is the latent heat of phase change, $174 kJ/kg$ for mineral oil.

Density $\rho(x, t)$ must be equal to the density of PMMA ρ_s while $T(x, t) < T2$ and equal to the density of air ρ_v when $T(x, t) > T2$. This is again specified using Heaviside step functions:

$$\rho(x, t) = \rho_s \times H(T_2 - T(x, t)) + \rho_v \times H(T(x, t) - T_2) \quad (8)$$

In this model, the sharp, discontinuous nature of the Heaviside function led to numerical instability. Instead, a continuously differentiable approximation was used:

$$H(z) \approx H_a(z, l) = 1 + \frac{1}{1 + e^{-2lz}} \quad (9)$$

where l is a user-defined constant. As $l \rightarrow \infty$, $H_a(z, l) \rightarrow H(z)$. For this work, $l = 0.5$ was found to give good results and be numerically stable. This function is coded in the script `smhv.m`.

In the substrate/PMMA system, ablation initiates at the surface (Figure 2). As time advances, the PMMA ablates further. The ablation tends to advance faster as the film becomes thinner due to reflected heat from the substrate/film interface.

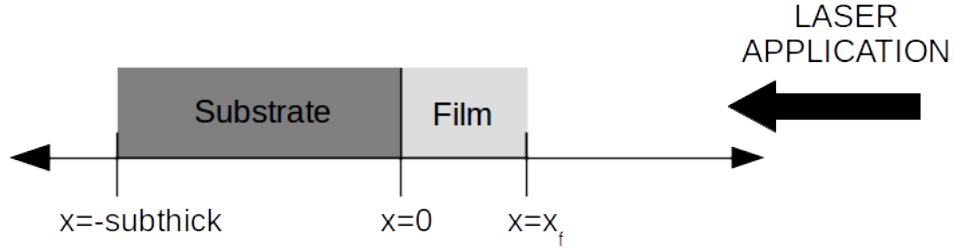


Figure 2: As time advances, the film ablates.

6 Thermal Energy Density and Flux

Thermal energy density was a quantity of interest in this work. The change in thermal energy density of a material is

$$de(x, t) = c(x, t)\rho(x, t)dT(x, t) \quad (10)$$

It was desired to compute thermal energy density at $x = 0$. Holding x and ρ constant, the total increase in thermal energy density at in the PMMA is

$$\Delta e(0, t) = \rho(0, T) \int_{25^\circ C}^{T(t)} c(0, T)dT \quad (11)$$

Holding ρ constant, Eq. 11 was numerically integrated in MATLAB to compute energy density. c was computed from Eq. 7

7 Results

Sample results are shown for a small model with the parameters given in Table 1. For additional information, the exact code run to obtain these results is given in `v7_pdepe.m`. This model took about 12 hours to run on a PC with 4x3GHz processors and 32GB of RAM.

Substrate Matl.	Carbon Steel
Substrate Height	1 μm
Film Matl.	PMMA
Film Height	1 μm
Laser	NdYAG
Fluence	100 mJ/cm^2
t_p	50 ns
Num. Pulses	5
Initial Temperature	25° C

Table 1: Model parameters for example results

Results showed ablation as expected. Phase change began at the surface heated by the laser, but heat clearly accumulated throughout the system during heating. Figure 3 shows temperature over all points and all timesteps. During the initial pulse heating, there is a rapid change in temperature in the PMMA. Then, between pulses, temperature evens out and equilibrates throughout the domain. Then, the next pulse ablates a bit more material, and so on. It is seen that temperature does not return to the ambient 25° C , but rather that heat accumulates in the system.

As phase change occurred in the film, it was seen that the film temperature reached a maximum of 475° as predicted. It may be instructive to take a closer look than can be seen in Figure 3. This progression of ablation can be seen during the first pulse in Fig. 4.

At the time that the third pulse is applied, considerable heat has accumulated in the material (Fig. 5). It can be seen that the amount of material where $T = 475^\circ$ is larger, indicating continuing ablation of the PMMA.

The increase in thermal energy density in the PMMA at the interface was tracked as well using Eq. 11. It is plotted in Figure 6.

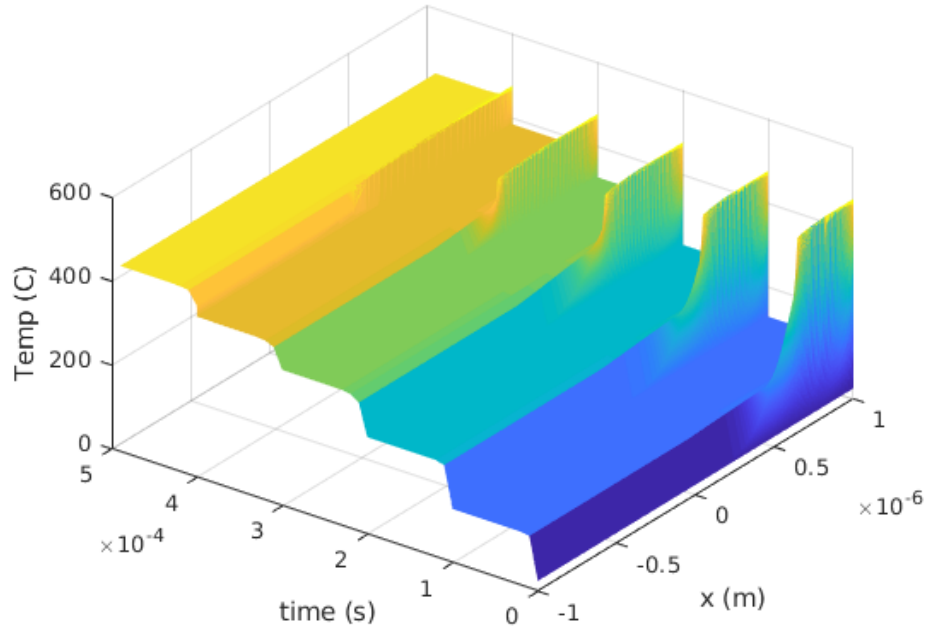


Figure 3: All results, all timesteps

Ablation of PMMA was also tracked and is shown in Figure 7. As expected, ablation occurs during pulses. Interestingly, the last pulse ablates more material than the two before it. This is presumably because as the PMMA vaporizes, the amount of energy reflected off the steel increases.

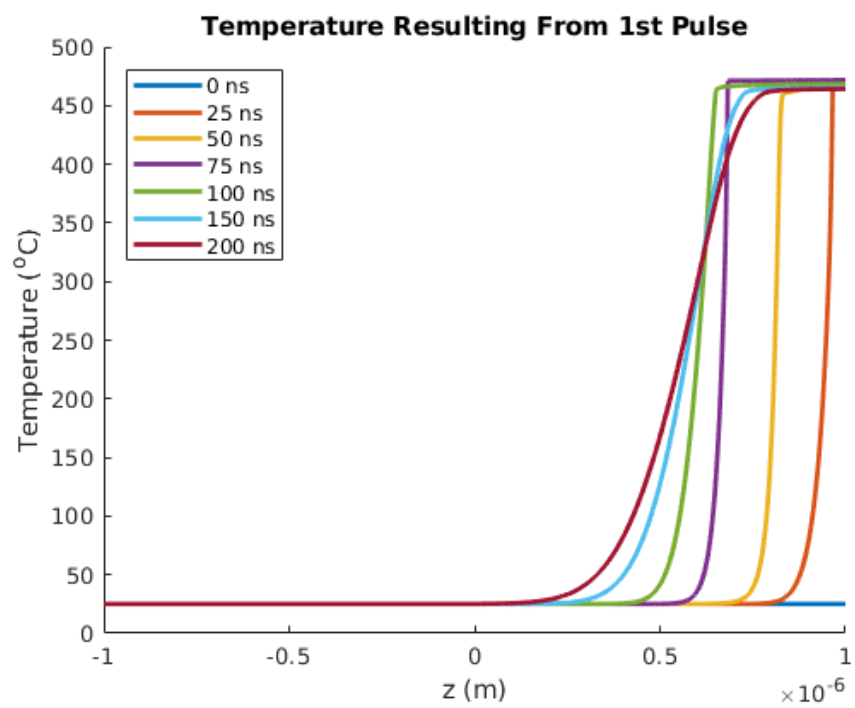


Figure 4: The flat portions of the temperature curve represent zones where the phase change has occurred.

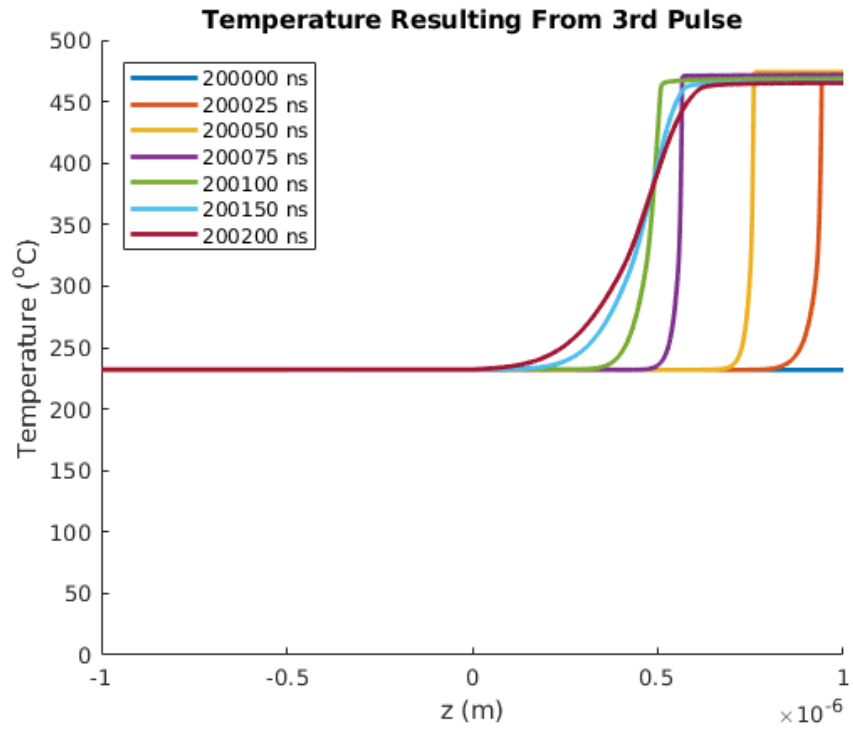


Figure 5: During and immediately after the 3rd pulse, temperatures are higher throughout the system. The amount of ablated material (where $T = 475^\circ$) is also greater than in the first pulse

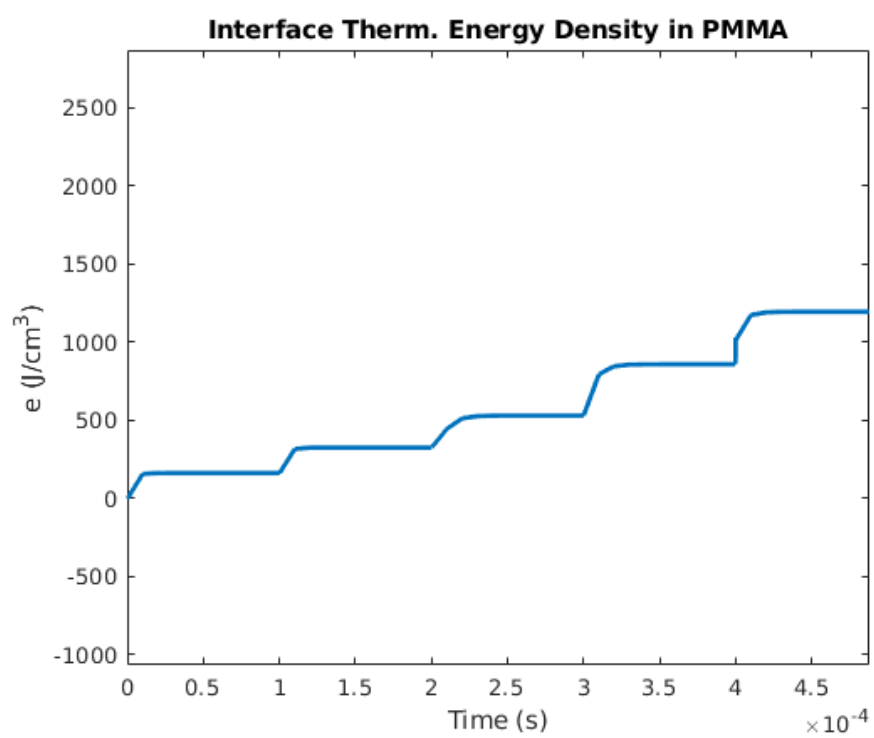


Figure 6: Increase in thermal energy density due to laser heating

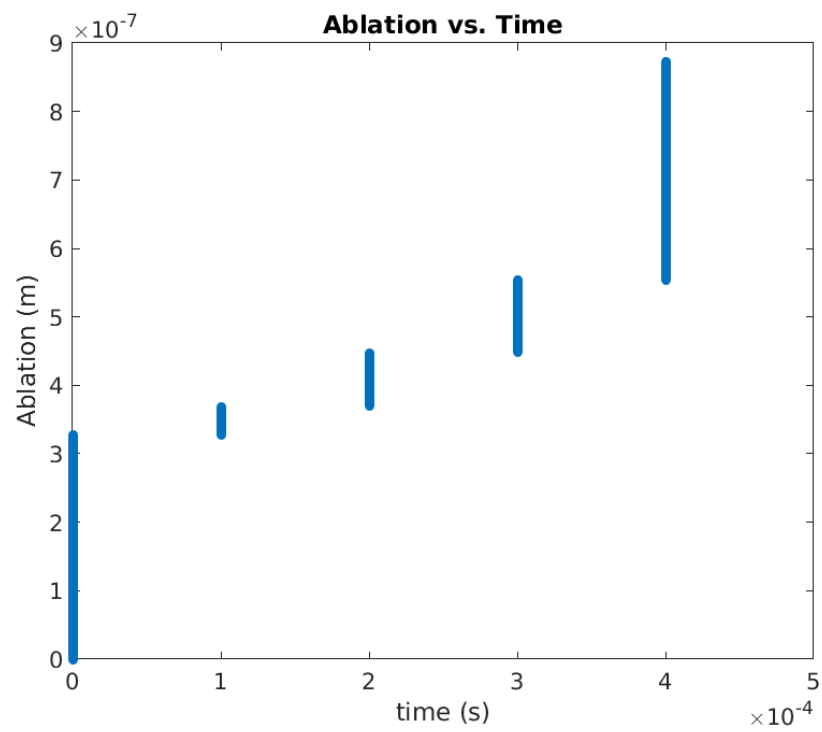


Figure 7: Ablation vs. time. The most material ablates during the first and last pulses.